Pseudo-invariants contributing to inverse energy cascades in three-dimensional turbulence

Nicholas M. Rathmann[*] and Peter D. Ditlevsen[†]

Niels Bohr Institute, University of Copenhagen, Copenhagen, Denmark

Three-dimensional (3D) turbulence is characterized by a dual forward cascade of both kinetic energy and helicity, a second inviscid flow invariant besides energy, from the integral scale of motion to the viscous dissipative scale. In helical flows, however, such as strongly rotating flows with broken mirror symmetry, an inverse (reversed) energy cascade can be observed analogous to that of two-dimensional turbulence (2D) where enstrophy, a second positive-definite flow invariant, unlike helicity in 3D, effectively blocks the forward cascade of energy. In the spectral-helical decomposition of the Navier-Stokes equation, it has previously been shown that a subset of three-wave (triad) interactions conserve helicity in 3D in a fashion similar to enstrophy in 2D, thus leading to a 2D-like inverse energy cascade in 3D. In this work, we show, both theoretically and numerically, that an additional subset of interactions exist, conserving a new pseudo-invariant in addition to energy and helicity, which contributes either to a forward or an inverse energy cascade depending on the specific triad interaction geometry.

I. INTRODUCTION

Fully developed three-dimensional (3D) turbulence is characterized by a forward cascade of kinetic energy from the large integral scale of motion to the small Kolmogorov scale η of viscous dissipation. In the large Reynolds number limit, $\eta \to 0$, the production of enstrophy, the integral of the vorticity squared, by the stretching and bending term in the incompressible Navier-Stokes equations (NSE) permits the viscous dissipation of energy at the Kolmogorov scale. In two-dimensional (2D) turbulence, the stretching and bending term is absent, and enstrophy is, in addition to energy, also an inviscid invariant [1]. In this case, the dissipation of enstrophy prevents dissipation of energy at the Kolmogorov scale, effectively blocking the forward cascade of energy. The dual inviscid conservation of both quantities, $\int E(k)dk$ and $\int k^2 E(k)dk$, the integrals over the spectral energy and enstrophy densities, respectively, consequently implies a reversal of the energy cascade to larger scales, hereafter referred to as a reverse cascade, following Waleffe [2] (synonymous to an inverse or upscale cascade). In 3D turbulence, helicity, the integral of the scalar product of velocity and vorticity, is also an inviscid invariant [3]. Similar to the enstrophy spectrum, the helicity spectrum, $H(k) \sim kE(k)$, dominates over the energy spectrum at small scales (large k), but unlike enstrophy, helicity is not sign definite. As a consequence, the increased dissipation (of both signs) of helicity compared to energy can be obtained without a net helicity production as long as the dissipation of both positive and negative helicities balance [4]. Inviscid conservation of helicity therefore does not prevent a forward cascade of energy [5].

In helical flows, such as strongly rotating flows with broken mirror symmetry, a simultaneous forward helicity cascade and reverse energy cascade can however be observed [6]. In the spectral decomposition of the NSE, energy and helicity (and enstrophy in 2D) are conserved within each three-wave interaction (triad interaction). It was recently proposed that reverse energy cascades might generally exist in 3D turbulence [7], caused by a specific subset of triad interactions among

---

[*]rathmann@nbi.ku.dk

[†]pditlev@nbi.ku.dk

054607-1
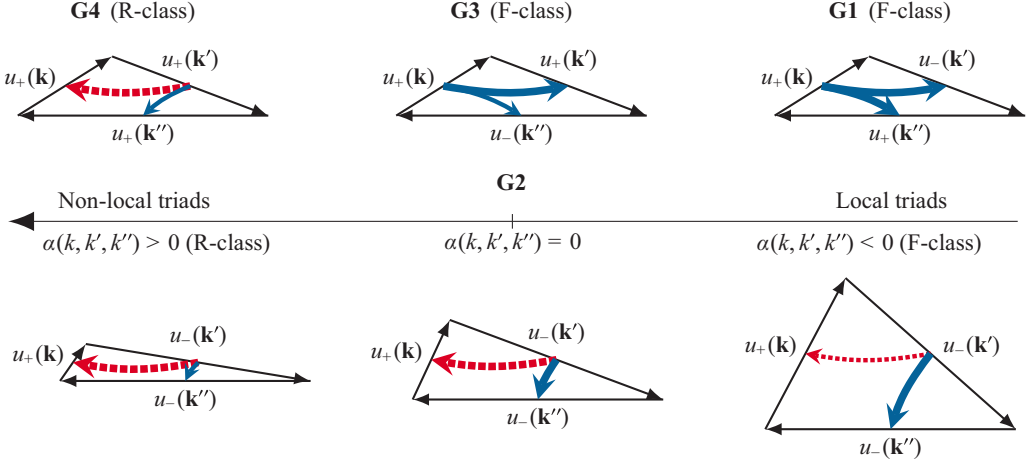
FIG. 1. G1–G4 helical triad interactions classified by behavior (F and R classes). The behavior of G2 triads is here proposed to be determined by the conservation of a new geometry-dependant enstrophy-like quantity, $E^{(\alpha)}$. The arrows indicate the average energy transfer directions based on a linear stability analysis [2]: Blue/solid (red/dashed) arrows denote forward (reverse) energy transfers while thick (thin) arrows represent the dominant (subordinate) transfers.

helical wave components [2] of the same sign which render helicity enstrophy-like. The relative roles played by the different of subsets of helical triad interactions would depend specifically on the symmetries and boundary conditions of the turbulent flow [8,9].

By applying the helical decomposition [2] to the NSE, triad interactions are split into four distinct groups of interactions between helical modes of different signs (depending on the relative weights of interchange of energy and helicity among the three waves). Within each helical interaction group, we show that an additional either helicity- or enstrophy-like quantity is conserved. Here, we conjecture that it is the spectral properties of this triad-specific invariant that governs the dual cascade of energy and helicity in 3D turbulence. Our conjecture is confirmed in the case of a shell model (reduced wave space model) which obeys the same conservations as the NSE [8].

In the helical decomposition [2] of the NSE for incompressible flows, each complex spectral velocity component, $\mathbf{u}(\mathbf{k})$, is decomposed into helical helical modes, $\mathbf{h}_{\pm}(\mathbf{k})$ (using $\mathbf{k} \cdot \mathbf{u}(\mathbf{k}) = 0$), which are eigenmodes of the curl operator, i.e., $i\mathbf{k} \times \mathbf{h}_{\pm} = \pm k\mathbf{h}_{\pm}$, where $k = |\mathbf{k}|$. In this basis, velocity components are given by $\mathbf{u}(\mathbf{k}) = u_{+}(\mathbf{k})\mathbf{h}_{+} + u_{-}(\mathbf{k})\mathbf{h}_{-}$, and energy and helicity are given by $E = \sum_{\mathbf{k}}(|u_{+}(\mathbf{k})|^2 + |u_{-}(\mathbf{k})|^2)$ and $H = \sum_{\mathbf{k}} k(|u_{+}(\mathbf{k})|^2 - |u_{-}(\mathbf{k})|^2)$, respectively. The spectral NSE become [2]

$$(d_t + \nu k^2)u_s(\mathbf{k}) = -1/4 \sum_{\mathbf{k}+\mathbf{k}'+\mathbf{k}''=0} \sum_{s',s''} (s'k' - s''k'') \mathbf{h}_{s'}^*(\mathbf{k}') \times \mathbf{h}_{s''}^*(\mathbf{k}'') \cdot \mathbf{h}_s^*(\mathbf{k}) u_{s'}^*(\mathbf{k}')u_{s''}^*(\mathbf{k}''), \quad (1)$$

where $\{s,s',s''\} = \pm 1$ are the helical signs of the interacting modes and $(s'k' - s''k'') \mathbf{h}_{s'}^*(\mathbf{k}') \times \mathbf{h}_{s''}^*(\mathbf{k}'') \cdot \mathbf{h}_s^*(\mathbf{k})$ is the coupling coefficient of the helical triad interaction involving velocity components $\{u_s(\mathbf{k}), u_{s'}(\mathbf{k}'), u_{s''}(\mathbf{k}'')\}$. Each triad interaction in the spectral NSE is thus split into four helical triad interactions by the inner sum over helical signs in (1) when sorted against shared coupling coefficients: $\{s,s',s''\} = \pm\{+,-,+\}, \pm\{+,-,-\}, \pm\{+,+,-\}, \pm\{+,+,+\}$, hereafter referred to as groups G1,. . .,G4 respectively; see Fig. 1.

By isolating terms in (1) involving only three wave vectors $\{\mathbf{k},\mathbf{k}',\mathbf{k}''\}$ (a single triad) and defining the shorthand notation $g = \mathbf{h}_{s'}^*(\mathbf{k}') \times \mathbf{h}_{s''}^*(\mathbf{k}'') \cdot \mathbf{h}_s^*(\mathbf{k})$, one finds, using the cyclic property

of g,

$$
\begin{aligned}
d_t u_s(\mathbf{k}) &= (s'k' - s''k'') \, g \, u_{s'}^*(\mathbf{k}')u_{s''}^*(\mathbf{k}''), \\
d_t u_{s'}(\mathbf{k}') &= (s''k'' - sk) \, g \, u_{s''}^*(\mathbf{k}'')u_s^*(\mathbf{k}), \\
d_t u_{s''}(\mathbf{k}'') &= (sk - s'k') \, g \, u_s^*(\mathbf{k})u_{s'}^*(\mathbf{k}').
\end{aligned}
\tag{2}
$$

This simple form of the helically decomposed NSE triad dynamics is the basis of our analysis. Note that the cyclic symmetry of (2) implies that one may assume $k \leqslant k' \leqslant k''$ without loss of generality. By multiplying by $u_s^*(\mathbf{k}), u_{s'}^*(\mathbf{k}')$ and $u_{s''}^*(\mathbf{k}'')$, respectively, in the three equations (2), it immediately follows that energy is conserved within each triad interaction, and similarly for helicity by multiplication of $sku_s^*(\mathbf{k}), s'k'u_{s'}^*(\mathbf{k}')$ and $s''k''u_{s''}^*(\mathbf{k}'')$, respectively [2]. The energy flux between the three triad legs is fixed for a given triad and is determined by the terms $(s'k' - s''k''), (s''k'' - sk)$, and $(sk - s'k')$ in (2), while the average flux direction (to or from a leg) is determined by the sign of the three-wave correlator $\langle u_s^*(\mathbf{k})u_{s'}^*(\mathbf{k}')u_{s''}^*(\mathbf{k}'')\rangle + \text{c.c.}$

Waleffe [2] suggested that a linear instability analysis would predict the average energy flux direction within helical triad interactions by assuming that energy, on average, flows out of the most unstable wave mode and into the other two. By evaluating the stability of the fixed points $\{u_s(\mathbf{k}), u_{s'}(\mathbf{k}'), u_{s''}(\mathbf{k}'')\} = \{U_0, 0, 0\}, \{0, U_0, 0\}, \{0, 0, U_0\}$ using (2), the unstable wave mode may be identified as the one with the largest absolute coefficient value in (2). This criterion implies that the smallest leg (largest scale) is unstable in G1 and G3 interactions, suggesting that these interactions contribute with a forward energy cascade (F-class interactions), while for G2 and G4 the middle leg is unstable, suggesting part of the energy flux is reversed. In G4, only same-signed helical modes interact, implying both positive and negative helicities, $H^+ = \sum_{\mathbf{k}} k|u_+(\mathbf{k})|^2$ and $H^- = \sum_{\mathbf{k}} k|u_-(\mathbf{k})|^2$), are separately conserved. As such, G4 interactions can be regarded as analogous to enstrophy-conserving 2D interactions, and, consequently, should contribute with a reversed energy cascade (R-class interactions). This was recently indeed found to be the case numerically [7]. Note that the 2D analogy argument for why G4 interactions should exhibit a reversed energy cascade is different from that of the instability assumption. Lastly, in G2 interactions, positive and negative helicity components do interact, thus breaking the helicity-enstrophy analogy for explaining the mixed F- and R-class nature of G2 [2].

II. THE PSEUDO-INVARIANT

Here we argue that the mixed F- and R-class nature of G2 interactions is determined by a new quantity different from energy and helicity, which too is conserved within a single triad interaction (2), but depends on triad shape. This new "pseudo-invariant" is thus, unlike energy and helicity, not a globally conserved quantity (across all triad interactions) because of its shape dependency. We therefore conjecture that the energy cascade, within subsets of identically shaped triads, should transition from forward (F-class) to reverse (R-class) depending on whether energy or the pseudo-invariant is dominant at the dissipation scale. To realize this, consider the spectral pseudo-invariant quantity defined as

$$
E^{(\alpha)}(\mathbf{k}) = k^\alpha \left(|u_+(\mathbf{k})|^2 + |u_-(\mathbf{k})|^2 \right), \quad \alpha \in \mathbb{R},
\tag{3}
$$

which is analogous to the spectral energy density $E(\mathbf{k}) = |u_+(\mathbf{k})|^2 + |u_-(\mathbf{k})|^2$. This quantity is conserved by triad interactions governed by (2) if $d_t(E^{(\alpha)}(\mathbf{k}) + E^{(\alpha)}(\mathbf{k}') + E^{(\alpha)}(\mathbf{k}'')) = 0$, implying

$$
\left(s'\frac{k'}{k} - s''\frac{k''}{k} \right) + \left(\frac{k'}{k} \right)^\alpha \left(s''\frac{k''}{k} - s \right) + \left(\frac{k''}{k} \right)^\alpha \left(s - s'\frac{k'}{k} \right) = 0,
\tag{4}
$$

which is trivially fulfilled for any triad when $\alpha = 0$ (i.e., energy). As a function of triad shape, given by the relative leg sizes k'/k and k''/k, the left-hand side of (4) consists of a constant term and two monotonically increasing or decreasing terms. The existence of a nontrivial, real solution ($\alpha \neq 0$)
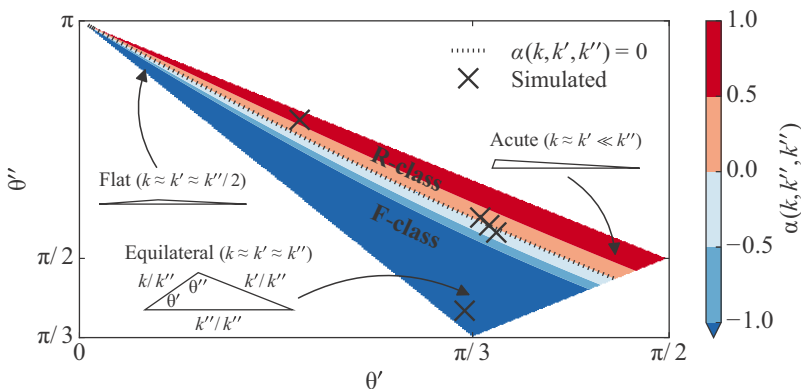
FIG. 2. G2 α solutions as a function of triad shape given by the two interior angles θ' and θ''. Overlayed are the $\alpha = 0$ contour using Eq. (5) (dotted line) and the specific triad geometries simulated in this study (crosses).

for a given triad shape $\{k, k', k''\}$ and interaction group $\{s, s', s''\}$ therefore requires the signs of the coefficients of the two last terms in (4) to be opposite. Note that no more than *one* nontrivial, real solution can exist. It follows that only G2 and G4 interactions can have nontrivial solutions to (4). For G4, $\alpha = 1$ is the solution for any triad, corresponding to the global inviscid conservation of helicity, as expected. For G2, the solution $\alpha = \alpha(k, k', k'')$ is triad shape dependent.

Figure 2 shows the numerically solved G2 solutions for all possible (noncongruent) triad geometries (colored area in Fig. 2) by expressing each triad in terms of the two interior angles θ' and θ'' using the sine rule: $k'/k = \sin(\theta')/\sin(\pi - \theta' - \theta'')$ and $k''/k = \sin(\theta'')/\sin(\pi - \theta' - \theta'')$.

For G2 triads fulfilling

$$\frac{\log k''/k}{1 + k''/k} = \frac{\log k'/k}{1 + k'/k}, \tag{5}$$

[taking $d/d\alpha|_{\alpha=0}$ of Eq. (4)], the trivial and nontrivial solutions collapse to the single solution $\alpha = 0$. Because the ratio of the spectral pseudo-invariant density to energy scales as k^α (growing with k for $\alpha > 0$), the subset of G2 triad interactions having $\alpha > 0$ (red in Fig. 2) may be regarded analogous to enstrophy-conserving interactions in 2D turbulence. Note that these triad interactions correspond to nonlocal interactions.

In addition to a stability analysis, Waleffe [2] also estimated the behaviors of G1–G4 by studying the spectral energy flux equation. Assuming an infinite Kolmogorov scaling, the analysis suggested, to leading order, that triad geometries for which

$$\frac{\log k/k'}{1 + k/k'} + \frac{\log k''/k'}{k''/k' - 1} \tag{6}$$

is positive (negative) should contribute with forward (reverse) energy cascades. Noting that $1 \leqslant k''/k' \leqslant k/k' + 1$ (triangle inequality), it follows that G2 triads with $k/k' > 0.318$ contribute to a forward cascade, whereas $k/k' < 0.278$ contribute reversely. That is, a band of triad geometries exist, $0.278 < k/k' < 0.318$, outside which the energy cascade is either forward or reverse. Here, however, we argue that retaining the original expression (6) contains more information on the G2 F/R transition since (i) setting it equal to 0 can be shown to be identical to (5), which has a clearer physical interpretation, and (ii) provides the exact F/R-transition line as a function of triad geometry (Fig. 2).

III. NUMERICAL TEST

In order to test our conjecture, we apply our newly constructed helical shell model [8] (source available at https://github.com/nicholasmr/rdshellmodel). Shell models are a class of fixed-triad-shape and reduced-wave-space models, allowing for very long inertial ranges to be resolved. Benzi *et al.* [10] did the pioneering work on constructing helical shell models, which, since then, has inspired other helical shell models and led to important insights on helically decomposed triad dynamics [4,8,11–17]. The shell model used here [8], which is related to the Sabra model [15] by the transformation $u_s(k_n) \rightarrow -isu_s(k_n)$ except for a sign change in G1 and G3 (relevant only when coupling G1–G4), additionally provides a natural coupling between the four interaction groups (G1–G4) and multiple triad shapes through coupling weights derived directly from (1).

In helical shell models, it is straightforward to perform "spectral surgery" as proposed [7,15,18,19] in order to investigate the (isolated/uncoupled) behavior of G2 interactions. Considering only fixed-shaped G2 interactions, the shell model takes the form

$$\left(d_t + \nu k_n^2 + \nu_L k_n^{-2}\right)u_s(k_n) = sk_n\left[u_{-s}^*(k_{n+p})u_{-s}(k_{n+q}) - \frac{\epsilon_{p,q}}{\lambda^p}u_{-s}^*(k_{n-p})u_s(k_{n+q-p}) \right.$$
$$\left. + \frac{1+\epsilon_{p,q}}{\lambda^q}u_{-s}(k_{n-q})u_s(k_{n-q+p}) \right] + f_s(k_n), \tag{7}$$

where $\epsilon_{p,q} = (1+\lambda^q)/(\lambda^p - \lambda^q)$, $f_s(k_n)$ is the forcing at wave number k_n, and the linear terms $\nu k_n^2 u_s(k_n)$ and $\nu_L k_n^{-2}u_s(k_n)$ are viscous dissipation and a drag term, respectively; the latter is added in the usual way to remove energy at large scales. The scalars $k_n = k_0\lambda^n$, where $n = 0, \ldots, N$, represent the exponentially distributed shell wave numbers resolved, $\{p,q\} \in \mathbb{N}$ where $1 < p < q$, $k_0 \in \mathbb{R}_+$, and $\lambda \in]1,(1+\sqrt{5})/2] =]1,\varphi]$. The golden ratio φ is the upper limit such that any set of nearest neighbor waves fulfills the triangle inequality as required by the NSE.

The integers $\{p,q\}$ can be related to any triangular shape through the sine rule. The possible resolved triad shapes depend therefore on the combination of $\{\lambda,p,q\}$: For $\lambda \rightarrow 1$ any triad geometry may be constructed for sufficiently large or small values of $\{p,q\}$, while for $\{\lambda,p,q\} = \{\varphi,1,2\}$ triads collapse to a line. Thus, for each chosen set of $\{\lambda,p,q\}$, the shell model consists, independently of scale k_n, only of fixed-shaped triad interactions.

The nonlinear terms in (7) conserve both energy $E = \sum_{n=0}^{N}(|u_+(k_n)|^2 + |u_-(k_n)|^2)$ and helicity $H = \sum_{n=0}^{N} k_n(|u_+(k_n)|^2 - |u_-(k_n)|^2)$. Each $\{p,q\}$ configuration of the model (λ hereafter assumed fixed) additionally conserves the pseudo-invariants $E^{(\alpha)} = \sum_{n=0}^{N} k_n^\alpha(|u_+(k_n)|^2 + |u_-(k_n)|^2)$ in complete analogy to (4) for the NSE [8].

The nonlinear spectral energy flux through the nth shell is given by [8]

$$\Pi(k_n) = \sum_{m=n+1}^{n+q} \Delta_{m,p,q} + \epsilon_{p,q} \sum_{m=n+1}^{n+q-p} \Delta_{m,p,q}, \tag{8}$$

where $\Delta_{m,p,q} = 2k_{m-q}\,\text{Re}[u_+^*(k_{m-q})u_-^*(k_{m-q+p})u_-(k_m) - u_-^*(k_{m-q})u_+^*(k_{m-q+p})u_+(k_m)]$.

Simulations were conducted with $\lambda = 1.1$, $k_0 = 1$, and $N = 223$ for both high and low Reynolds number configurations $\{\nu, \nu_L\} = \{1\times10^{-12},\, 1\times10^2\}$, $\{1\times10^{-11},\, 1\times10^4\}$, respectively. Five different sets of $\{p,q\}$ were chosen: $p = \{1,12,13,14,22\}$ with $q = p+1$, corresponding to $\alpha = \{-30.9, -0.15, 0.01, 0.15, 0.69\}$ (crosses in Fig. 2). In all simulations, the forcing $f_\pm(k_{n_f}) = (1+i)/u_\pm^*(k_{n_f})$ was applied to both helical components at shell $n_f = 108$, supplying a constant energy input of $\epsilon_{in} = 4$.

Figure 3 shows the simulated spectral energy fluxes. The blue curves show the resulting energy fluxes for the model configured with triad shapes having $\alpha < 0$, in which case energy should exhibit a forward cascade. The red curves show the opposite with $\alpha > 0$, namely a 2D-like reversed energy cascade and a forward cascade of the enstrophy-like pseudo-invariant (latter not shown). As the
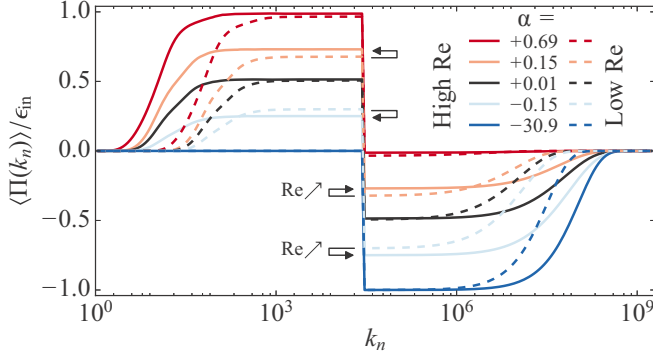
FIG. 3. Simulated spectral energy fluxes of the G2 triad geometries (α values) considered. Solid (dashed) lines correspond to high (low) Reynolds number configurations.

cascade directions for the energy and the pseudo-invariant interchange at $\alpha = 0$, we expect a split forward and reversed energy cascade to develop, which is indeed found to be the case (black curve in Fig. 3). Furthermore, because the ratio of the spectral pseudo-invariant density to energy scales as k^α, one would expect with increasing Reynolds numbers a narrowing of the α interval over which the F- to R-class transition occurs, which is also found to be the case (solid versus dashed lines in Fig. 3).

IV. DISCUSSION

De Pietro *et al.* [15] gave an alternative explanation for the F to R transition in the case of a shell model by studying the energy flux equation (8). Their work suggested that if time-averaged triple correlators, $\langle \Delta_{n,p,q} \rangle$, are asymptotically constant (independent of k_n), Eq. (8) may be written as $\langle \Pi(k_n) \rangle = (q + (q - p)\epsilon_{p,q})\langle \Delta_{n,p,q} \rangle = F_{p,q}\langle \Delta_{n,p,q} \rangle$. Thus, the sign of $F_{p,q}$, which depends on triad geometry, would indicate the flux direction, assuming the sign of $\langle \Delta_{n,p,q} \rangle$ is fixed and given by a stability analysis [2,15]. However, even though this prediction is in agreement with our conjecture for the triad geometries considered here, it is important to note that $\langle \Delta_{n,p,q} \rangle$ cannot necessarily be assumed asymptotically constant in the nonlocal triad limit [8].

The importance of the "hidden" reverse energy cascade carried by G2 R-class interactions ($\alpha > 0$), which are mostly nonlocal, depends (i) on the number of G2 R-class triads compared to the number of G2 F-class triads, and (ii) the magnitude of the G2 coupling coefficients in (1) compared to those of G1, G3, and G4. To estimate (i), consider the continuous version of (1) where the triad sum becomes an integral over $dk'dk''$. In terms of θ' and θ'', the corresponding density of triads within the element $dk'dk''$ is given by the transformation $dk'dk'' = |\det J| \, d\theta' d\theta''$, where $J = \partial \Phi$ is the Jacobian of the transformation $k' = \Phi'(\theta', \theta'')$ and $|\det J| = k^2 \sin(\theta') \sin(\theta'')[1 + \cos(\theta' + \theta'')^2]/\sin(\theta' + \theta'')^4$. Thus, the number of G2 R-class triads far exceeds the number of G2 F-class triads in the limit of large inertial ranges (Re $\to \infty$) since the acute triad limit $k', k'' \to \infty$ implies $\sin(\theta' + \theta'') \to 0$ and therefore a large density of nonlocal triads. To estimate (ii), consider the relative (normalized) magnitudes of the G2 coupling coefficients given by $I_{-,-}/\sum_{s',s''} I_{s',s''}$, where $I_{s',s''} = |(sk + s'k' + s''k'')(s'k' - s''k'')|$. That is, $I_{s',s''}$ is the part of the total coupling weight unique to each of G1–G4, which originates from (1) by noting $|(s'k' - s''k'') \, g| = I_{s',s''} Q/(2kk'k'')$, where $Q = (2k^2k'^2 + 2k'^2k''^2 + 2k''^2k^2 - k^4 - k'^4 - k''^4)^{1/2}$ [2]. Figure 4 shows the relative G2 coupling magnitudes (solid black lines), suggesting G2 R-class interactions should, overall, play an important role in the helically decomposed dynamics of flat and semi-acute triads. In addition, assuming $k = 1$ without loss of generality, the colored contours in Fig. 4 show the triad density, $|\det J|$, is also large for such flat and semi-acute triads triads, suggesting G2 R-class interactions
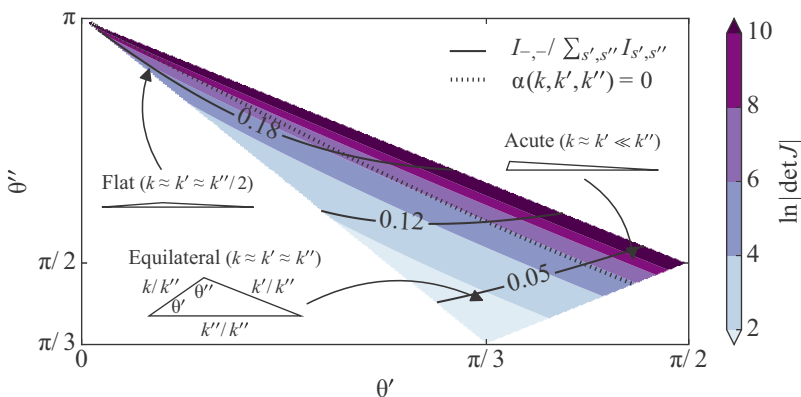
FIG. 4. G2 relative coupling weight (solid black contours) and triad densities (coloured contours) as a function of triad shape.

become increasingly important to the extent that the inertial range is long enough for them to be resolved.

V. SUMMARY

In conclusion, we presented an alternative classification to linear triad stability analysis [2] for explaining the nature of the four elementary nonlinear interactions of the spectral Navier-Stokes equation in the helical basis. By showing a subset of interactions conserve new enstrophy-like blocking quantities depending on triad geometry, the apparent complicated nature of the second group (G2) of helical interactions (Fig. 1) may be explained in terms of physically conserved quantities analogous to enstrophy in 2D turbulence.

---

[1] R. H. Kraichnan, Inertial ranges in two-dimensional turbulence, Phys. Fluids **10**, 1417 (1967).

[2] F. Waleffe, The nature of triad interactions in homogeneous turbulence, Phys. Fluids **4**, 350 (1992).

[3] H. K. Moffatt, The degree of knottedness of tangled vortex lines, J. Fluid Mech. **35**, 117 (1969).

[4] P. D. Ditlevsen and P. Giuliani, Dissipation in helical turbulence, Phys. Fluids **13**, 3508 (2001).

[5] A. Brissaud, U. Frisch, J. Leorat, M. Lesieur, and A. Mazure, Helicity cascades in fully developed isotropic turbulence, Phys. Fluids **16**, 1366 (1973).

[6] P. D. Mininni, A. Alexakis, and A. Pouquet, Scale interactions and scaling laws in rotating flows at moderate rossby numbers and large reynolds numbers, Phys. Fluids **21**, 015108 (2009).

[7] L. Biferale, S. Musacchio, and F. Toschi, Inverse Energy Cascade in Three-Dimensional Isotropic Turbulence, Phys. Rev. Lett. **108**, 164501 (2012).

[8] N. M. Rathmann and P. D. Ditlevsen, Role of helicity in triad interactions in three-dimensional turbulence investigated by a new shell model, Phys. Rev. E **94**, 033115 (2016).

[9] A. Alexakis, Helically decomposed turbulence, J. Fluid Mech. **812**, 752 (2017).

[10] R. Benzi, L. Biferale, R. M. Kerr, and E. Trovatore, Helical shell models for three-dimensional turbulence, Phys. Rev. E **53**, 3541 (1996).

[11] P. D. Ditlevsen and P. Giuliani, Cascades in helical turbulence, Phys. Rev. E **63**, 036304 (2001).

[12] T. Lessinnes, F. Plunian, and D. Carati, Helical shell models for MHD, Theor. Comput. Fluid Dyn. **23**, 439 (2009).

[13] T. Lessinnes, F. Plunian, R. Stepanov, and D. Carati, Dissipation scales of kinetic helicities in turbulence, Phys. Fluids **23**, 035108 (2011).

[14] R. Stepanov, P. Frick, and I. Mizeva, Joint inverse cascade of magnetic energy and magnetic helicity in mhd turbulence, Astrophys. J. Lett. **798**, L35 (2015).

[15] M. De Pietro, L. Biferale, and A. A. Mailybaev, Inverse energy cascade in nonlocal helical shell models of turbulence, Phys. Rev. E **92**, 043021 (2015).

[16] G. Sahoo, M. De Pietro, and L. Biferale, Helicity statistics in homogeneous and isotropic turbulence and turbulence models, Phys. Rev. Fluids **2**, 024601 (2017).

[17] M. De Pietro, A. A. Mailybaev, and L. Biferale, Chaotic and regular instantons in helical shell models of turbulence, Phys. Rev. Fluids **2**, 034606 (2017).

[18] L. Biferale, S. Musacchio, and F. Toschi, Split energy–helicity cascades in three-dimensional homogeneous and isotropic turbulence, J. Fluid Mech. **730**, 309 (2013).

[19] G. Sahoo, F. Bonaccorso, and L. Biferale, Role of helicity for large- and small-scale turbulent fluctuations, Phys. Rev. E **92**, 051002(R) (2015).